

A Comparison between One and Two Component Velocity and Size Measurements in a Dense Spray

M. Mojtabi¹, G. Wigley^{1*}, J. Jedelsky² and J. Helie³

¹ Aero and Auto Engineering, Loughborough University, LE11 3TU, UK

² Faculty of Mechanical Engineering, Brno University of Technology, Czech Republic

³ Continental Automotive SAS, BP 1149 Toulouse Cedex 1, France

Abstract

Dense spray streams produced by a three hole gasoline direct injector have been characterised in the near nozzle region using single shot CCD imaging and the phase Doppler technique in one and two component velocity configuration. The conclusion reached was that one component measurements in dense sprays provide the better estimates for droplet size.

Introduction

PDA measurements in the near nozzle regions of transient hollow cone high pressure swirl GDI fuel sprays have been attempted successfully [1]. Imaging of the spray with the input laser beams identifies the bulk spray morphology, the spray density, the propagation of the input laser beams and the location of the PDA measurement volume. It was revealed that the major problem to obtaining successful PDA data in the near nozzle region of the hollow cone spray was the obscuration of the input beams when the measurement volume was aligned with the inside surface of the spray cone when the input laser beams would be obscured before the crossover. When the measurement volume is positioned on the spray cone centre line multiple scatter from droplets and remnants of the liquid sheet in, or near, the measurement volume results in a significantly reduced signal validation rate, the effects of which could be reduced by increased data acquisition times [1].

The probability of successful PDA measurements can be increased by minimising the dimensions of the measurement volume, maximising the probability of laser beam crossover and droplet detection and performing preliminary measurements to establish the trade off between increasing the ‘system gain’ and optical noise break through on the data. Reducing a PDA system configuration from two component to one component velocity provides another option for maximising the probability of the formation of the laser beam crossover albeit at the cost of reducing the full measurement potential.

Materials and Methods

The two component PDA system and atmospheric spray rig and its application to GDI fuel sprays have been well documented [1] and [2]. The multi-hole injector was supplied by Continental Automotive, however, whereas normal production injectors would have a 6 hole nozzle this was made to provide only three nozzles. The advantage for this study is that the input laser beams only interact with the spray stream under analysis. A schematic is shown in Figure 1.

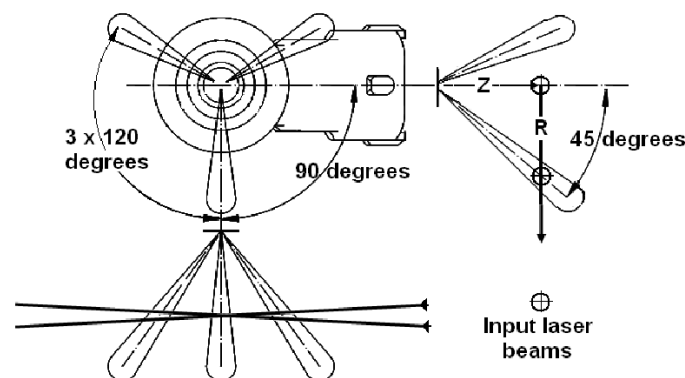


Figure 1. Injector spray geometry and PDA laser beam alignment

* Corresponding author: g.wigley@lboro.ac.uk

The three-hole GDI injector was supported from a gantry incorporating a rotation stage and three precision orthogonal linear traverses to orientate and position the spray in three dimensions relative to the static PDA measurement volume. Each radial scan started from the geometric vertical axis through the nozzle tip and traversed out to the periphery of the spray stream. The measurement co-ordinates in the vertical plane were $Z = 3, 5, 7.5$ and 10 mm below the nozzle tip. The horizontal traverse was computer controlled and programmed with a radial step increment of nominally 10% of the Z value in order to resolve local high velocity gradients across the cone of the spray stream in the horizontal plane. A much coarser grid was possible near the spray stream axis as no droplets at all were found, i.e. there was no interaction between the spray streams.

In order to quantify the interaction of the spray cone angle with the input laser beams and PDA measurement volume, single-shot images were digitally recorded with a PCO Sencicam Fast Shutter CCD camera equipped with a Nikon 55 mm focal length macro lens. The focus for the lens was the vertical plane through the input laser beams i.e. the injector axis for $R = 0$ mm. The camera provided an image size of approximately 50 by 40 mm, represented by 1280 by 1024 pixels. The injector control unit provided electronic triggers, referenced to the opening pulse of the injector solenoid, which, through a variable delay unit, controlled both the flash and image capture time. The time delay was fixed at 2 ms, i.e. the same time that the injector was programmed to close. Five images were stored for each radial traverse position to allow an evaluation of shot to shot variations and a mean image to be created to highlight how the bulk features of the spray stream interacted with the input laser beams. Imaging was vital to ensure that the centre of the spray stream passed symmetrically through the PDA laser cross over volume.

The injector was fuelled with 95 RON unleaded gasoline with a fuel line pressure of 100 bar pressure. The injection pulse duration time was 3 ms comprising of 1 ms soak time and 2 ms fuel delivery. The injected fuel mass was 9 mg/ms. The injection frequency was 4 Hz. A single shot and mean image are shown in Figure 2 with the laser beams at $Z = 5$ mm and $R = 6.5$ mm, the radius corresponding to maximum axial velocity. The intensity profile of the laser beam interaction with the spray stream certainly indicates significant obscuration to the formation of the measurement volume, particularly in the single shot case. Laser beam direction is from right to left.

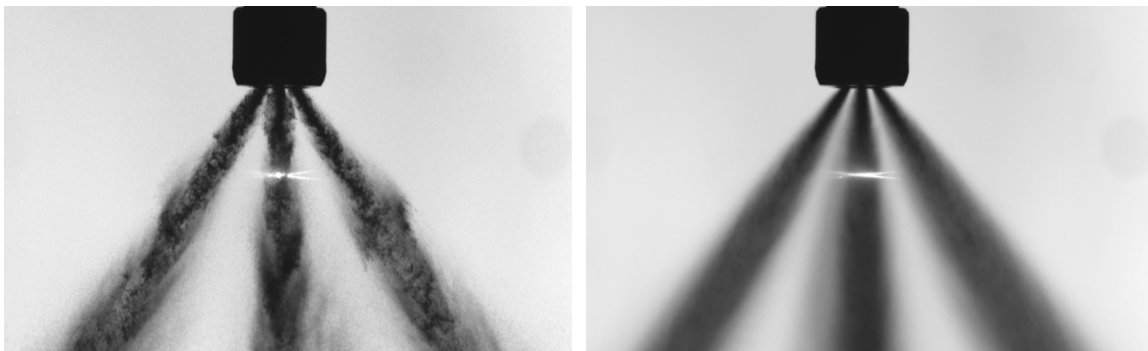


Figure 2. Single shot, left, and mean image, right, showing spray stream -laser beam interaction

The two component configuration for the 488 and 514 nm laser beam wavelengths at the final focussing lens was: beam diameters of 5 mm, equal beam pair separations of 50 mm, laser powers of 100 and 200 milli-watts per beam, and, with a focal length lens of 300 mm produced coincident measurement volumes of diameters of 56 and 59 microns with fringe spacings of 3.10 and 2.94 microns respectively for the two wavelengths. This produced an experimental velocity bandwidth of nominally -40 to 110 m/s.

The standard Dantec 57X10 receiver optical system was positioned at a scattering angle of 70 degrees with an aperture micrometer setting of 0.5 mm. This optical configuration resulted in an effective measurement volume length of 0.1 mm and a maximum drop size measurement range of up to 100 microns. The Dantec PDA covariance processor was set to acquire validated data samples at each measurement position for a fixed acquisition time of 50 seconds i.e. for 200 injections. Two component coincidence is forced since the signal processor has only one burst detector, on the axial 514 nm channel, and the measurement volume for the radial component, 488 nm, is nearly 10% smaller. A fixed acquisition time allows a better estimate of spray stream density from the droplet sample number collected.

Measurement scans for the one and two component data were made sequentially and, with a total acquisition time of less than 15 minutes per scan, ensured minimum variations in environmental conditions for the spray. Since the Dantec covariance processor only has a burst detector on the 514 nm sizing channel two component data are only valid with essentially true coincidence of the signals in each channel.

Once the radial location for the maximum axial velocity in each scan across the spray stream had been determined the PDA measurement volume was re-located at the $Z = 3, 5$ and 7.5 mm locations and single point measurements for the 1D and 2D PDA configuration were taken sequentially with a 100 second acquisition time.

This obviously doubled the amount of data allowing statistically significant probability density functions of dropsize to be produced while ensuring that the radial location was identical in each case.

Results and Discussion

The 1D and 2D PDA data selected to be presented are, firstly; the time resolved droplet velocity and size corresponding to the radial location at which the maximum axial velocity was recorded at the nearest distance from the nozzle and, secondly; the spatial variations over a fixed time period, relating to near steady state conditions, for the axial mean and rms velocity, the arithmetic mean diameter D_{10} and the distribution of data sample number for all the measurement planes.

The raw axial velocity and dropsize data are presented in Figure 3 for the measurement point $Z = 3$ mm at $R = 4.5$ mm where the maximum axial velocity was recorded, this is termed the spray stream axis. The droplet data for the 1D and 2D cases are in the upper and lower plots respectively. The greater data density for the 1D case is obvious with a total of 17967 samples being recorded when compared to 12847 for the 2D case. The origin for the time history is the electronic start of injection, ESOI, and is followed by the 1 ms soak time for the injector solenoid. The 0.2 ms before any data samples are seen is due to the injector response time and the time of flight of the spray stream from the injector to the measurement point 3 mm downstream and 4.5 mm radially. From the velocity data it can be seen that the transient leading edge of the stream has passed through after a further 0.6 ms, i.e. 1.8 ms after ESOI when a near steady state condition is established until 3.4 ms after which the spray stream velocity decays rapidly as the needle starts to close. Shortly before 4 ms there appears a small peak in the axial velocity which correlates with a substantial increase in the detection of larger dropsizes. This is certainly due to the release of a small amount of fuel caused by a rebound of the injector needle.

Mean axial velocity and drop diameter, D_{10} , profiles are plotted on top of the raw data using a moving average of 300 samples in order to try and capture the velocity transients. The profiles are quite comparable between the two measurement cases and with the different data densities in the raw data plots it is also difficult to spot any significant differences between the two measurements.

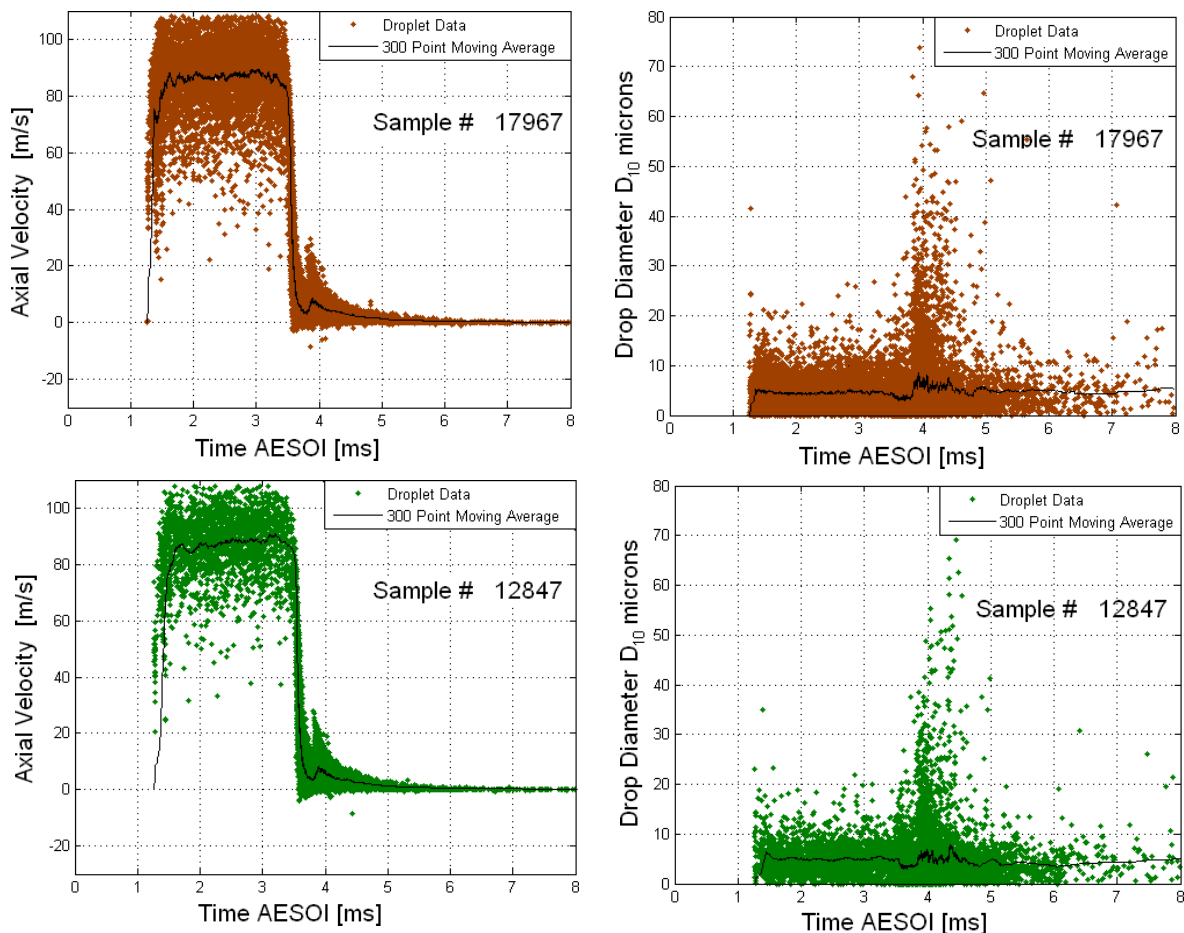


Figure 3. 1D (upper) and 2D (lower) raw velocity and dropsize data at $Z = 3$ mm and $R = 4.5$ mm

Since the actual injection period of 2 ms is relatively long, time bins of 0.50 ms have been used to produce the time varying mean profiles of the data and the following analysis only takes into account the quasi steady state period of the spray. The radial profiles of the droplet size D_{10} are shown in Figure 4 for the Z levels of 3 and 5 mm over the time bin 2.0 to 2.5 ms after ESOI. The profiles have a W shape with larger droplets found in the perimeter of the spray stream and along its axis, while the smaller droplets are to be found in the regions of greatest shear as will be shown later in Figure 6.

Considering that the 1D and 2D measurements were made sequentially the agreement between the profiles is very good except along the spray stream axis where the 2D data can be considered to overestimate the droplet size by nominally 2 and 1 microns at Z = 3 and 5 mm respectively. To examine the reasons for this the droplet size PDFs, with 0.5 micron size classes, are plotted for the 1D and 2D cases in the lower and upper plots respectively. In order to have statistically significant sample numbers and identical spatial location of the measurement volume on the spray stream axis these data have come from the single point measurement series apart from the data for Z = 10 mm. As the data were taken over a fixed time the sample numbers forming the droplet size PDFs are different, accordingly the 1D PDFs have been weighted with the ratio of the 1D/2D sample numbers.

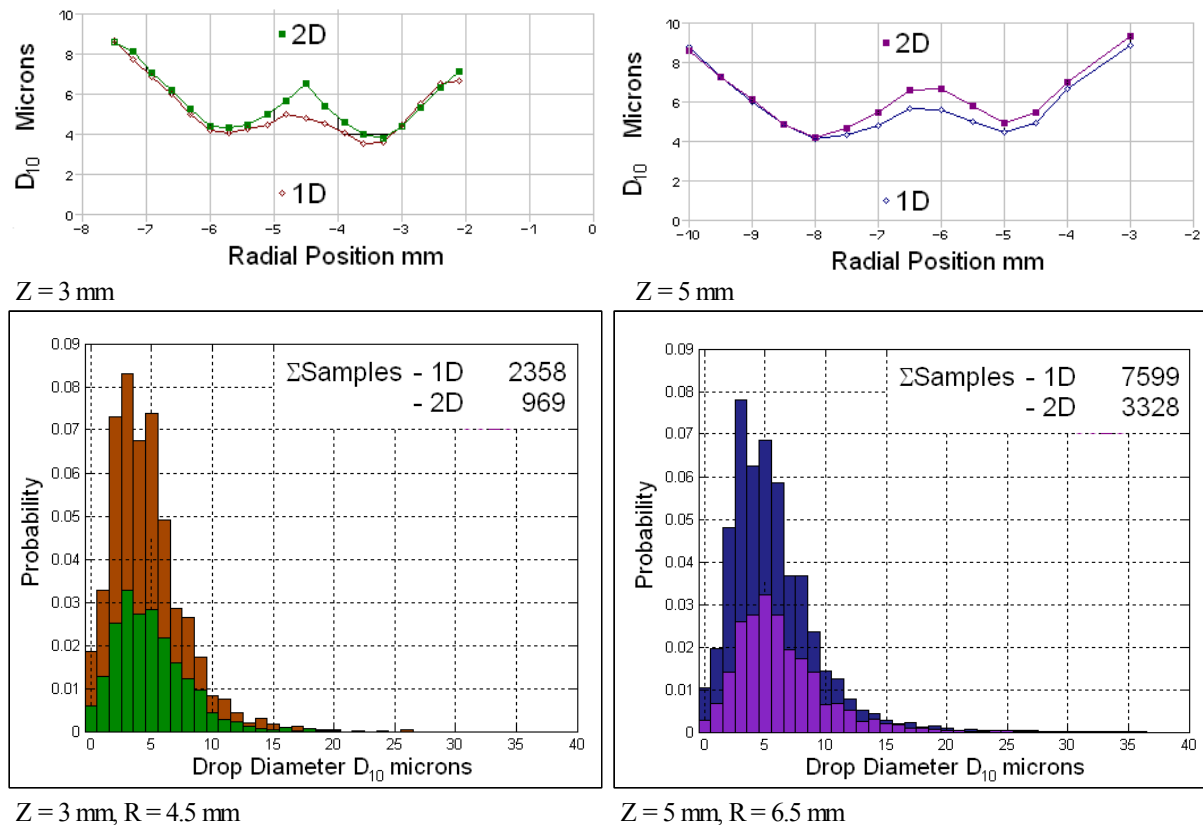


Figure 4. Radial profiles of droplet size at Z = 3 and 5 mm with the corresponding PDF at the stream axis

The superposition of the PDFs readily shows that in the 2D case far fewer sample numbers have been acquired. The average ratio of 2D to 1D counts is 40 % and 45 % for Z = 3 and 5 mm respectively. However, in the size classes below 5 microns the ratio is less, while above 5 microns, the ratio improves slightly. For the size classes in excess of 10 microns the differences decrease even more, especially as the size range increases with increasing Z value. For Z = 5 mm and R = 6.5 mm both the 1D and 2D cases are showing droplet sizes of up to 35 microns while in the Z = 3 mm plane the maximum droplet sizes seen were ~25 microns. This is consequence of moving further down the primary break up zone into regions where the liquid fuel elements are starting to break up.

This gradual improvement in validated sample numbers with increasing droplet size signifies that the reduced beam quality does not lead to a simple exclusion of the lowest sizes.

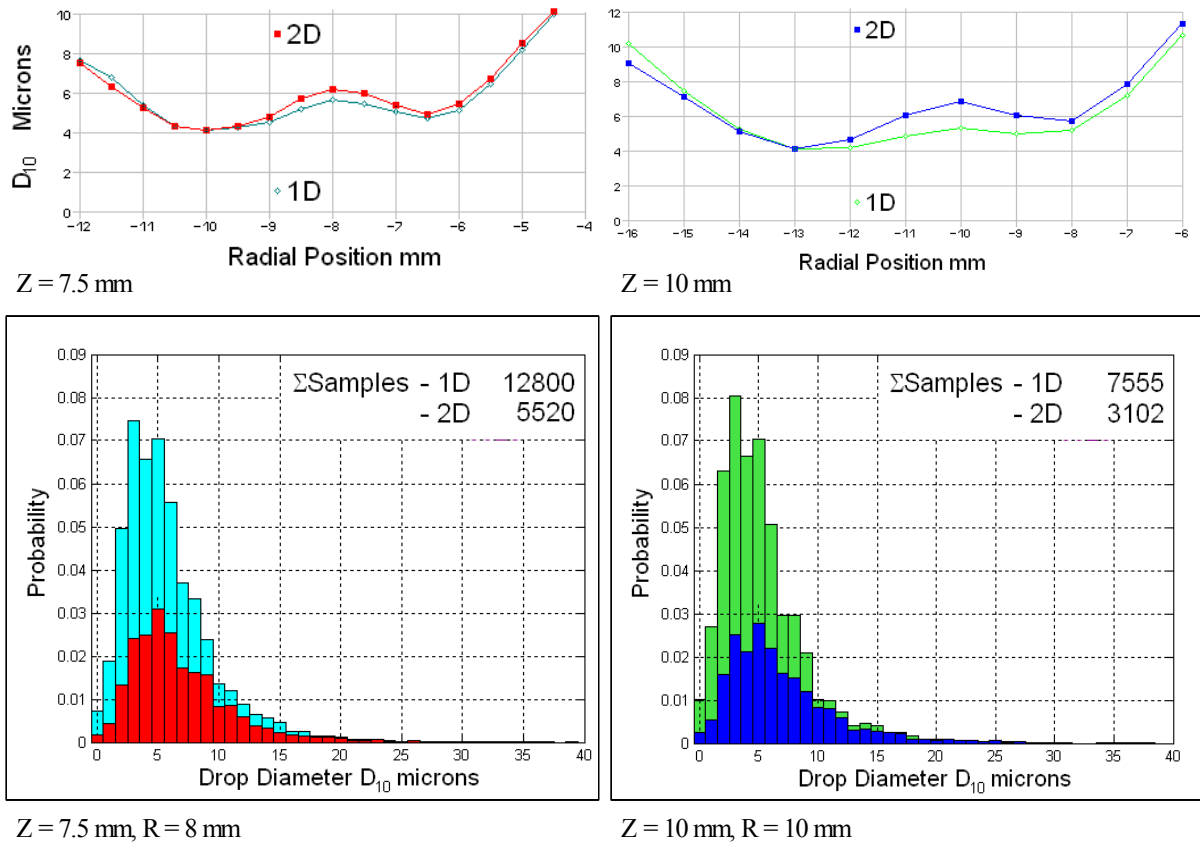


Figure 5. Radial profiles of dropsize at Z = 7.5 and 10 mm with the corresponding PDF on the stream axis

This trend is readily seen in the PDFs in Figure 5 where the sample numbers in the 1D and 2D cases start to converge from Z = 7.5 to 10 mm while the overall ratio of samples is 43 % and 41 % respectively. The sample numbers for Z = 10 mm are reduced as the data come from the 50 second 200 injection experimental series. As a consequence of the convergence of the sample numbers for dropsize classes in excess of 10 microns comes an increase in the Sauter mean diameters as calculated for the 2D case when compared to the 1D case as can be seen in Table 1.

Table 1. Comparison of Sauter mean diameters for the 1D and 2D cases as a function of Z plane

Coordinates mm	Sauter mean Diameter - 1D microns	Sauter mean Diameter - 2D microns
Z = 3 R = 4.5	8.81	8.80
Z = 5 R = 6.5	11.66	16.51
Z = 7.5 R = 8	14.68	15.25
Z = 10 R = 10	13.43	16.91

By configuring the PDA system in one component maximises the probability of the formation of the laser beam crossover and therefore detection of the smaller dropsize classes. The above attempts to quantify the effect of PDA system configuration on the estimates of the dropsize. The following now considers the effects on the velocity field and numbers of acquired samples. Radial profiles of the mean and fluctuating, RMS, components of the droplet axial velocity across the spray stream for the Z planes are shown in Figure 6. The data come from the 50 second, 200 injections experiment. The negative coordinates are a function of the traverse system with the spray axis to the right of each plot. For Z = 5, 7.5 and 10 mm the plots are offset from the spray centreline. The profiles highlight the radial growth of the spray stream downstream from the nozzle being 5.4, 7.0, 7.5 and 10 mm wide at Z = 3, 5, 7.5 and 10 mm respectively as primary break up progresses rapidly.

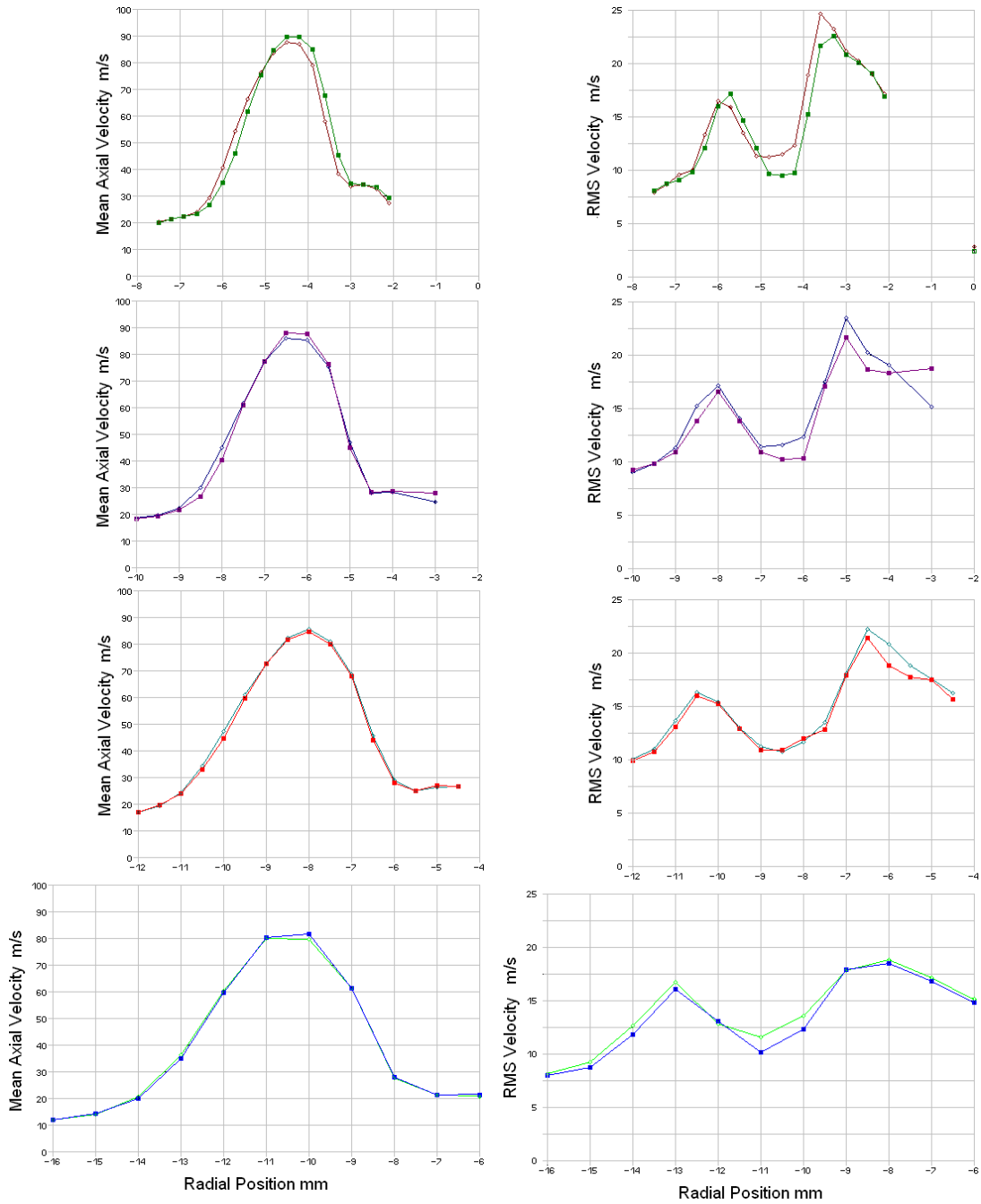


Figure 6. Radial profiles of axial mean and RMS velocities at $Z = 3, 5, 7.5$ and 10 mm

The colour coding of the profiles is the same as for the data shown in Figures 4 and 5. In all cases, the maxima in axial velocities and their corresponding minima in the RMS values on the spray axis are obtained for the 2D PDA system configuration. However, the differences in the mean velocity profiles on the spray axis between the 1D and 2D cases are small, especially for $Z = 7.5$ and 10 mm, with only a 2 % difference at $Z = 3$ mm. The differences are consistent with the differences in droplet size data where the 2D data record the higher droplet size measurements by discriminating against the small droplet size classes which would be travelling more slowly than the larger drops.

The axial velocity and RMS profiles are not symmetrical with higher mean and RMS velocities on the inside edge of the spray stream. This is a consequence of the orifice being bored at 45 degrees incidence to the injector nozzle face. The inside edge of the spray stream has the highest shear gradient and hence highest RMS values. With increasing Z the peak in the RMS values decreases consistently to approach the values on the outer spray stream edge.

There does appear to be a shift radially, to the left, in the 1D velocity profile compared to the 2D case. However, at 0.3 mm, one measurement point, this is small, however, such a shift would not be consistent with

the data profiles in the edges of the stream in both the mean and RMS profiles as well as the sample number profiles shown in Figure 7.

The sample number profiles for the 1D and 2D cases are easily discernable as the latter have generally far fewer samples. The profiles mimic those for the RMS velocity; low, but with near equal values, in the outer edges of the spray stream, rising in the shear layers with maximum momentum transfer and then dipping towards the spray axis. The location of the minimum sample numbers are displaced towards the inner edge of the locations for the maximum velocity and minimum RMS values.

In the plane $Z = 3$ mm the lowest sample numbers recorded are due to the nature of the primary break up process on the spray axis where large fluid elements have a much greater disruption on the integrity of the measurement volume. The inequality of the sample numbers on the inside edge of the spray axis is probably due to the extra optical path length for the scattered light to reach the receiver. Since the sample numbers for the 1D and 2D cases are quite similar in the peak, representing the outer limit of the shear regions, then it would suggest that obscuration and hence droplet production is low.

Droplet production along the spray axis will improve as the primary break up nears completion and this is seen as a large increase in the sample numbers. However, with an increasing spray width comes an increase in the optical length in the spray. Even at $Z = 20$ mm downstream the peak sample detected numbers is not on the spray axis. The wider shear layer on the outer edge of the stream is also considered responsible for beam obscuration and hence the much lower sample counts for the 2D case.

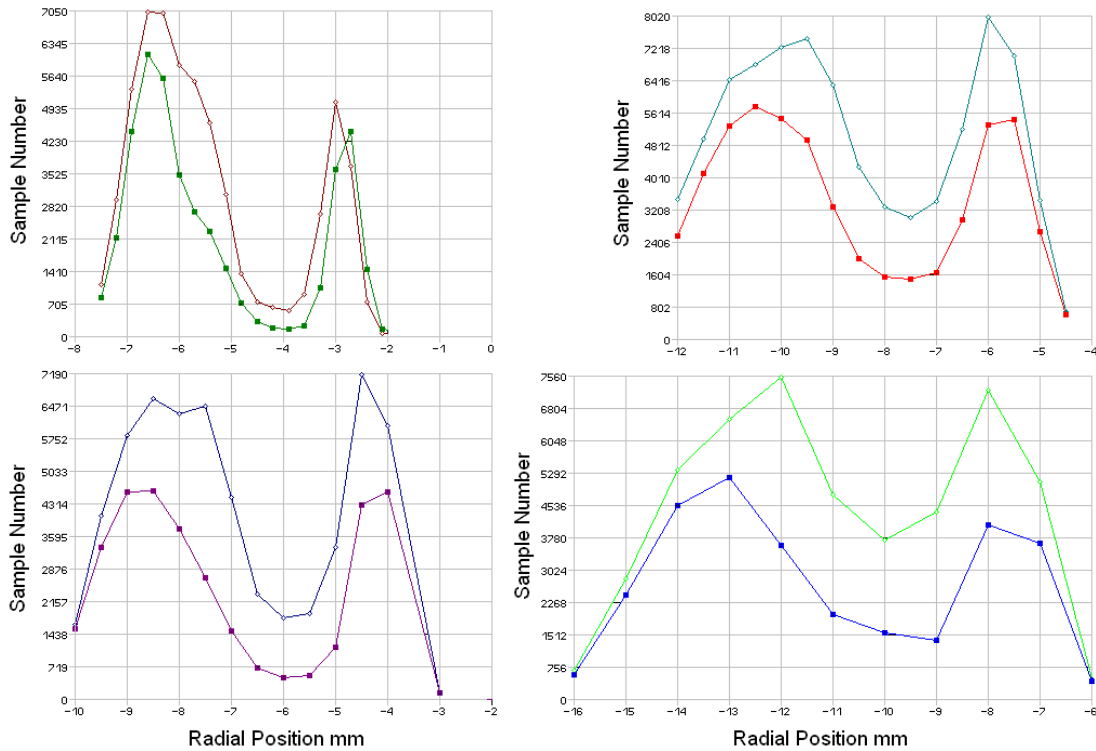


Figure 7. Radial profiles of sample numbers at $Z = 3$ and 5 mm (left) and 7.5 and 10 mm (right)

The final discussion in this comparison of 1D and 2D measurements relates to the information given by the processor as regards its validation performance during the measurements along the spray axis. Although these data are not available for the specific time period of the above data the overall values can be used as the 2 ms injection period will have the dominating influence over the transient start and collapse of the spray. The validation set up was quite strict with a signal validation level of 0 dB and with maximum phase and spherical error levels of 7 %.

The validation data presented in Figure 8 show the number of samples attempted (right hand scale), validated and spherical (left hand scale) i.e. the number of times the burst detector was triggered, the number passing the signal level criteria on the one, or two, channels and the number finally accepted with consistent phase estimates between the signals from the three detectors.

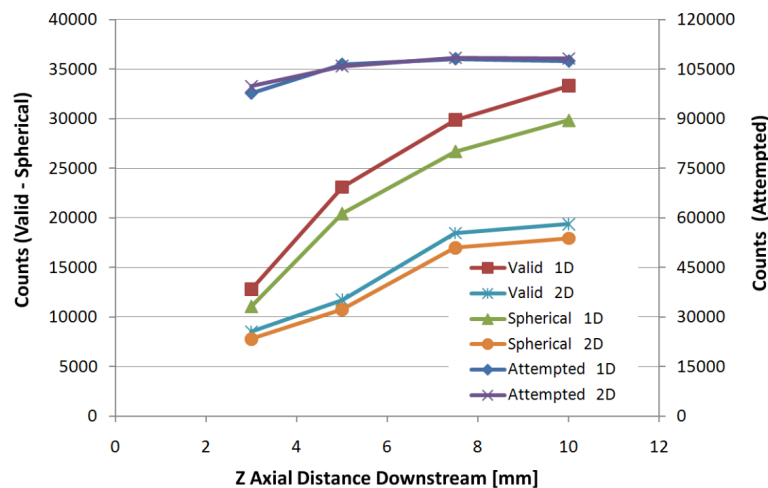


Figure 8. Validation profiles for the 1D and 2D cases as a function of axial distance

Interestingly, the number of times that the burst detector was triggered successfully is, apart from $z = 3$ mm, highly consistent with distance down the spray axis. As the response of the processor is not the limiting factor it must relate to the transport of similar numbers of scatterers between one position to the next.

The validation in the 1D case is seen to improve more rapidly than the 2D case with increasing distance downstream, with an overall validation percentage approaching 30 % of the burst detector triggers. However, the difference between the level and consistent phase validations is smaller for the 2D case. With the extra validation criteria to be met for a 2D measurement it obviously forces a higher probability of true droplet detection with the overall validation percentage level approaching 16 % at $Z = 10$ mm downstream from the nozzle.

This detailed analysis of velocity and droplet size measurements made with 1D and 2D PDA system configurations in the primary break up region of the dense spray produced by a GDI multi-stream injector has attempted to quantify the effects caused by laser beam and measurement volume obscuration. The special 3 hole injector allowed one particular spray stream to be studied without any interference from the other streams while maintaining stream similarity with a conventional 6 hole injector. The probability of only two laser beams crossing in the spray and generating a valid signal is significantly greater for the 1D system. This is readily seen in the sample number plots where, in some cases sample numbers can be a factor of two larger and this gives the velocity and droplet size data greater statistical significance.

The 1D configuration also provides better estimates of the smaller size classes but it was found that reduced beam quality does not lead to a simple exclusion of the lowest sizes. Effectively all sizes below 10 microns would be discriminated against. Whereas this affects the arithmetic mean values the Sauter mean values are less affected.

Where the droplet velocities are concerned there are only small differences in the profiles across the spray stream, at the 2 % level, between the 1D and 2D systems. The overall conclusion is that for dense sprays a 1D PDA system configuration provides the best estimates of sample number, droplet velocity and size with a 2D configuration providing adequate estimates of the droplet trajectory.

References

- [1] Pitcher, G., Wigley, G. and Stansfield, P.A., "Interpretation of Phase Doppler Measurements in a Dense Transient Fuel Spray", *13th International Symposium on Applications of Laser Techniques to Fluid Mechanics*, Lisbon, Portugal, 26-29 June, 2006.
- [2] Wigley, G., Pitcher, G., Nuglisch, H., Helie, J. and Ladommatos, N. "Fuel Spray Formation and Gasoline Direct Injection", *AVL 8th. International Symposium on Combustion Diagnostics*, Baden-Baden, Germany, 2008.